doi:10.1017/S1431927621010278
Microsc. Microanal. 27 (Suppl 1), 2021

Modeling and characterization of binder jet 3D printed NiMnGa components using X-ray microscopy

Stephen Isacco[1], Bartlomiej Winiarski[2], Christopher Bansah[3], Matthew Caputo[4] and Constantin V. Solomon[3]

[1]Youngstown State Univeristy, Youngstown, Ohio, United States, [2]Thermo Fisher Scientific, United States, [3]Youngstown State University, Youngstown, Ohio, United States, [4]PennState Shenango, Sharon, Pennsylvania, United States

Binder jetting additive manufacturing provides major benefits for obtaining NiMnGa components displaying magnetic shape memory effect (MSME) [1-3]. In the case of NiMnGa alloys it was proved that cast porous materials with bimodal pore-size distributions shows a magnetic field induced strain (MFIS) up to 8.7% [4]. Increased MFIS in porous polycrystalline NiMnGa, compared to the bulk material, was explained by the reduced constraints imposed by grain boundaries, thus enabling twin boundary motion [5]. However, obtaining NiMnGa foams by casting proved to be a complicated manufacturing technique, which offers limited capabilities in producing parts with complex geometry. Caputo *et al.* [6] proposed a simple technological approach to obtain porous polycrystalline NiMnGa components with any desirable shape, by taking advantage of the inherent porosity presented in parts produced by powder bed binder jetting additive manufacturing.

The purpose of using X-ray microscopy in this investigation was to visualize the structure of additive manufactured NiMnGa component, in order to obtain a true solid body for the numerical modeling on part's mechanical behavior. The true solid body will include manufacturing defects and imperfection, thus eliminating some geometrical errors inherent to the modeling process when using computer generated geometries. The quantification of pore-size distribution was also of interest, since it affects both the MFIS in polycrystalline NiMnGa parts, as well as the structural resistance, including the fatigue behavior and failure mechanism of the 3D printed component. Therefore, in order to understand the functional and structural behavior of additive manufactured NiMnGa components the X-ray microscopy data is quintessential in obtaining an operational computer model that will mimic and match the experimental behavior.

For this work, cubes with a gyroid cellular structure and an edge length of 4 mm, Fig. 1 (a), were manufactured in an ExOne X1-Lab binder jet printer [6, 7]. After printing the cubes were cured in air at 190˚C for 4 hours and then sintered at 1080˚C for 8 hours in argon. X-ray microscopy of sintered parts was performed in a HeliScanmicroCT, Thermo Scientific. The voxel sizes used in scanning the samples was 2.25 µm. Uniaxial compressive testing of sintered samples was performed using an Instron 5967 testing machine equipped with a 10 kN load cell following ASTM E9-89a standard recommendations. Sample displacement during compressive testing was quantified by digital image correlation using video tracking (Opti-TekScope

https://doi.org/10.1017/S1431927621010278 Published online by Cambridge University Press

OT-V1) and MatLab image processing. Fractured surface investigation was preformed using a JEOL JSM-7600F SEM.

The three-dimensional model of the gyroid sample, in the STL file format, was reconstructed from the micro-CT slices using Avizo software (Thermo Fischer Scientific). Unconstrained smoothing function was applied in order to create smooth surfaces and simplify the model. A solid body was obtained from the STL file using FreeCAD and SolidWorks software (Dassault Systems). Mechanical behavior of the additive manufactured part was investigated by finite element analysis. Simulations were done with ANSYS Mechanical, under transient structural, with time steps set to 0.1 s over 10 s.

The sintered NiMnGa gyroid cube obtained by binder jet 3D printing is shown in Figure 1 (a). The micro-CT scan of the component is shown in Figure 1 (b). The compressive stress nephogram indicated that the maximum equivalent (von Mises) stress was 3633.6 MPa, Figure 1 (c). This stress is much higher than the compressive fracture stress obtain experimentally which is about 110 MPa, Figure 1 (c). The difference can be explained by examining the submodels extracted from the model in Figure 1 (c) and presented in Figure 2 (d) and (e). The stress sharply increases at the sinter necks which act as stress raisers, due to their specific geometry. Based on the obtained data, the stress concentration factor for a sinter neck is $k_t \approx 33$. The numerical compressive stress-strain behavior of the 3D printed gyroid cube overlaps the experimental behavior, to a certain extent. It must be noted that the compressive behavior of the binder jet 3D printed and sintered NiMnGa component is similar to the mechanical behavior of single crystal NiMnGa actuator [8]. The initial linear compressive stress-strain behavior is related to the elastic deformation of martensite. When the stress reaches about 75 MPa, the material stiffness sharply decreases due to the mobility of the twin boundaries in the martensite. The twin boundary reorientation ends at about 85 MPa, and further stress increase yields elastic strain only.

Figure 2 (a) shows the 3D printed NiMnGa gyroid cube toward the end of the compressive test, as indicated by the longitudinal crack observed in the sample. The crack propagation path was observed by X-ray microscopy, Figure 2 (b), and SEM investigation of the fracture surface, Figure 2 (c). Submodels extracted from the model in Figure 1 (c) show the highest compressive stresses at edge of sinter necks, Figure 2 (d) and (e). Therefore, the sinter neck it is expected to be the crack initiation site during compressive testing. This was confirmed by the SEM investigation of the fracture surface, Figure 2 (f). As indicated by the red arrows, the cracks start at sinter necks and then propagated throughout the component.

https://doi.org/10.1017/S1431927621010278 Published online by Cambridge University Press

In conclusion, the X-ray microscopy provided an accurate solid body for the numerical modeling of the mechanical behavior of binder jet 3D printed NiMnGa component.

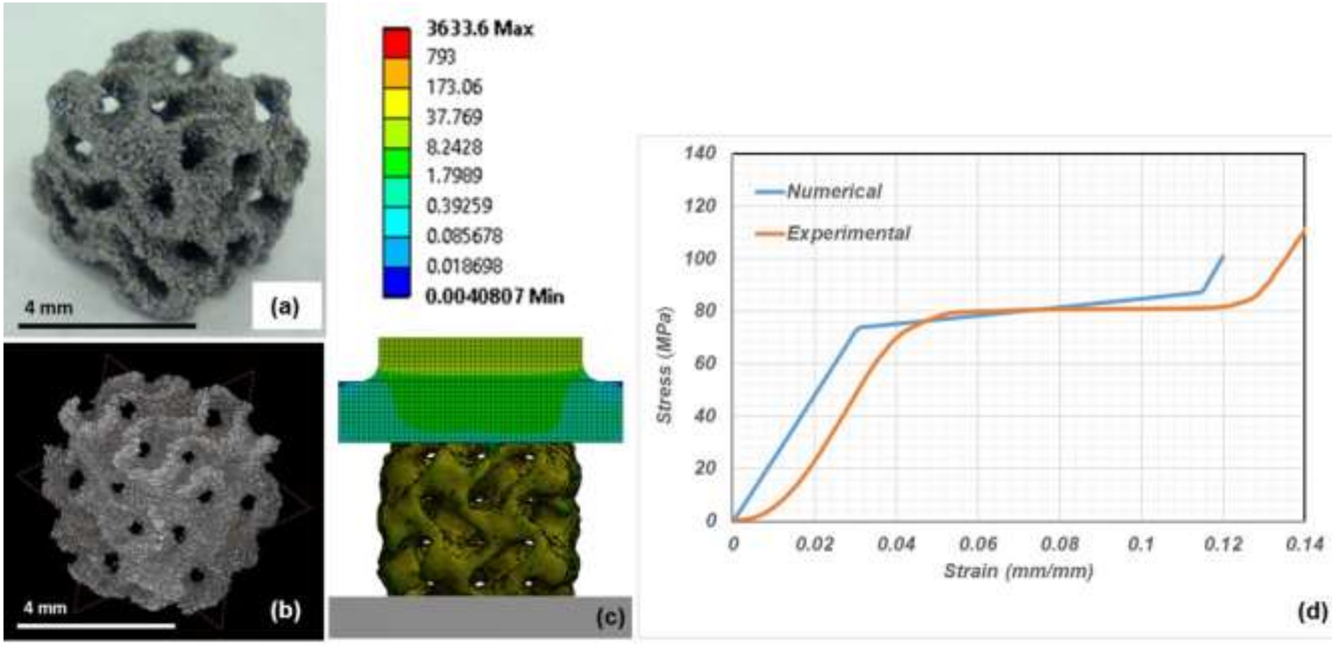

Figure 1. (a) Sintered NiMnGa gyroid cube obtained by binder jet 3D printing; (b) Micro-CT scan of the gyroid cube; (c) Stress nephogram of the component under compression load. The scale indicates the equivalent (von Mises) stresses developed in the model, in MPa; (d) Compressive strain-stress plots obtained via laboratory testing and numerical modeling.

https://doi.org/10.1017/S1431927621010278 Published online by Cambridge University Press

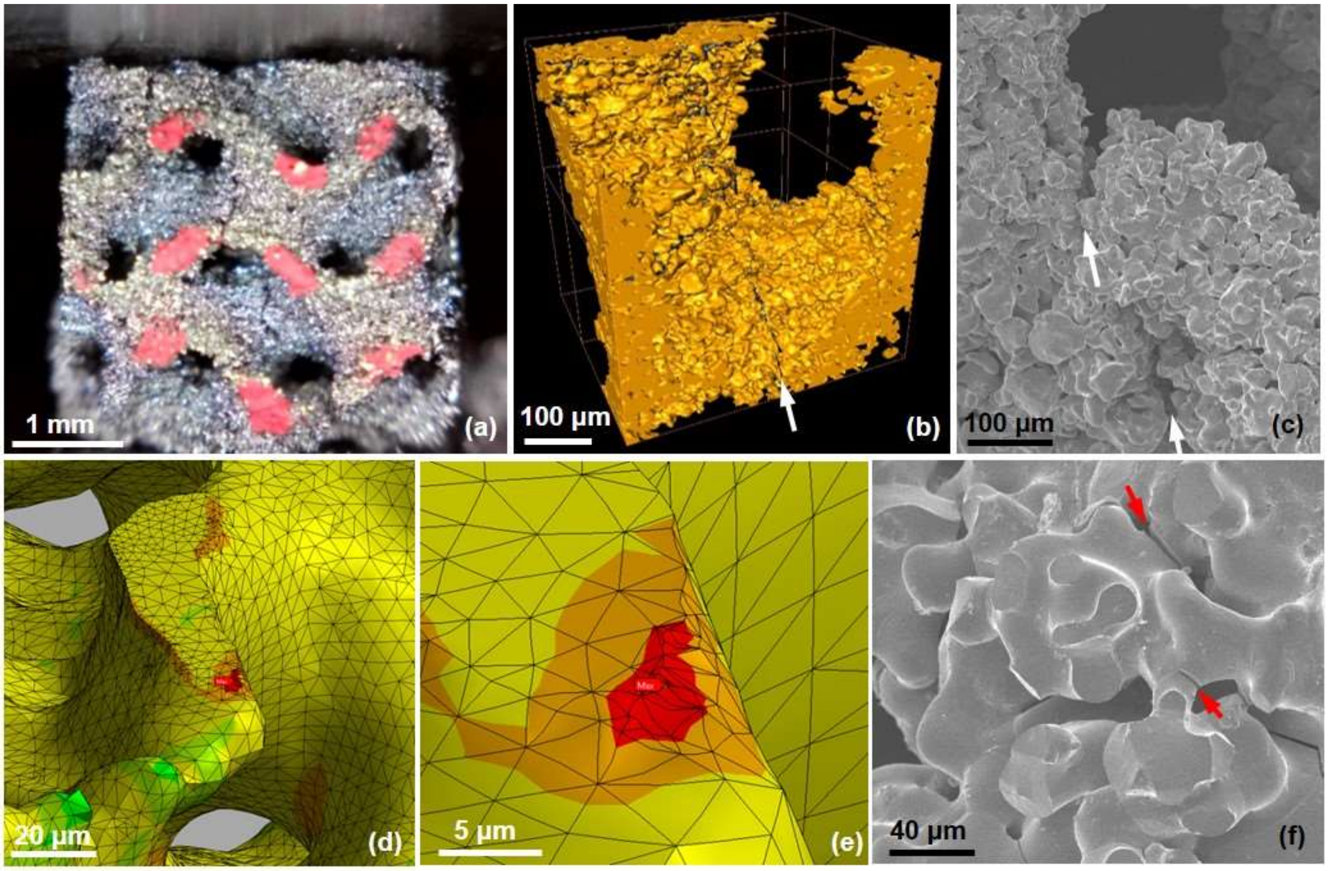

Figure 2. (a) 3D printed NiMnGa gyroid cube during compressive testing; (b) 3D rendering of a region of interest in the additive manufactured component, containing a longitudinal crack (indicated by the white arrow); (c) Secondary electron micrograph of the fracture surface of a compressed sample; (d), (e) Submodels extracted from the model in Figure 1 (c) showing high stresses at sinter necks; (f) Secondary electron micrograph of the fractured sample showing the crack initiation and propagation across sinter necks (red arrows).

References

[1] A. Mostafaei, K.A. Kimes, E.L. Stevens, J. Toman, Y.L. Krimer, K. Ullakko, and M. Chmielus, Microstructural evolution and magnetic properties of binder jet additive manufactured Ni-Mn-Ga magnetic shape memory alloy foam, Acta Mater. 131 (2017) 482 – 490.

[2] M.P. Caputo, A.E. Berkowitz, A. Armstrong, P. Muller, and C.V. Solomon, 4D printing of net shape parts made from Ni-Mn-Ga magnetic shape memory alloys, Additive Manufacturing 21 (2018) 579 – 588.

[3] M. Caputo, C.V. Solomon, P. Nguyen, and A.E. Berkowitz, Electron microscopy investigation of binder saturation and microstructural defects in functional parts made by additive manufacturing, Microsc. Microanal. 22 (2016) 1770 –1771.

[4] M. Chmielus, X.X. Zhang, C. Witherspoon, D.C. Dunand, P. Müllner, Nat. Mater. 8 (2009) 863 – 866.

[5] D.C. Dunand and P. Müllner, Size effect on magnetic actuation in Ni-MN-Ga shape-memory alloys, Adv. Mater. 23 (2011) 216 – 232.

https://doi.org/10.1017/S1431927621010278 Published online by Cambridge University Press

[6] M.P. Caputo, C.V. Solomon, A facile method for producing porous parts with complex geometries from ferromagnetic Ni-Mn-Ga shape memory alloys, Mater. Lett. 200 (2017) 87–89.
[7] M.P. Caputo, D.R. Waryoba, and C.V. Solomon, Sintering effects on additive manufactured Ni–Mn–Ga shape memory alloys: a microstructure and thermal analysis, J Mater Sci 55 (2020) 5311–5321, https://doi.org/10.1007/s10853-020-04352-9.
[8] R.N. Couch and I. Chopra, A quasi-static model for NiMnGa magnetic shape memory alloy, Smart Mater. Struct. 16 (2007) S11.